AIAA JOURNAL
Vol. 42, No. 5, May 2004

Actual Impedance of Nonreflecting Boundary Conditions: Implications for Computation of Resonators

Laurent Selle*
Centre Européen de Recherche et de Formation Avancée en Calcul Scientifique, 31057 Toulouse, France
Franck Nicoud†
University Montpellier II, 34095 Montpellier Cedex, France
and
Thierry Poinsot‡
Institut de Mécanique des Fluides, Toulouse, 31400 Toulouse, France

Nonreflecting boundary conditions are essential elements in the computation of many compressible flows. Such simulations are very sensitive to the treatment of acoustic waves at boundaries. Nonreflecting conditions allow acoustic waves to propagate through boundaries with zero or small levels of reflection into the domain. However, perfectly nonreflecting conditions must be avoided because they can lead to ill-posed problems for the mean flow. Various methods have been proposed to construct boundary conditions that can be sufficiently nonreflecting for the acoustic field while still making the mean flow problem well-posed. A widely used technique for nonreflecting outlets is analyzed (Poinsot, T., and Lele, S., "Boundary Conditions for Direct Simulations of Compressible Viscous Flows," *Journal of Computational Physics*, Vol. 101, No. 1, 1992, pp. 104–129; Rudy, D. H., and Strikwerda, J. C., "A Non-Reflecting Outflow Boundary Condition for Subsonic Navier–Stokes Calculations," *Journal of Computational Physics*, Vol. 36, 1980, pp. 55–70). It shows that the correction introduced by these authors can lead to large reflection levels and resonant behavior that cannot be observed in the experiment. A simple scaling is proposed to evaluate the relaxation coefficient used in these methods for a nonreflecting outlet. The proposed scaling is tested for simple cases (ducts) both theoretically and numerically.

I. Introduction

DERIVING nonreflecting boundary conditions for hyperbolic or incompletely hyperbolic problems[1] is a key problem in multiple fields such as classical engineering fluid dynamics,[2–8] aeroacoustics,[9–12] astrophysics,[13–15] vibrations in solids,[16] and electromagnetism.[17]

In the field of fluid mechanics, acoustic phenomena can affect the flow in a drastic manner in potentially unstable cases.[18–20] The numerical simulation of such flows in compressible codes is a major issue. Numerical boundary conditions must be treated with great caution to predict both the acoustic waves and the mean flow. Even though techniques have been developed to predict the mean flow in steady compressible codes (when acoustic phenomena are suppressed by numerical or physical viscosity) or to control the acoustic waves in linearized codes (where the mean flow is imposed), no method can handle both the mean flow and the acoustic waves in a perfect way: boundary conditions that allow perfect control of the mean flow generally reflect acoustic waves, whereas purely nonreflecting conditions used, for example, for linearized simulations allow mean flow values to drift.

One example where such issues are critical is the prediction of combustion instabilities in reacting flows.[20–24] Flames exhibit strong combustion instabilities when they are placed in channels. These oscillations are due to coupling between the flame and the channel acoustics (Fig. 1a). Acoustic waves are reflected at inlets and outlets into the domain where they can couple with the hydrodynamics and the unsteady heat release. A convenient method for characterizing these instabilities is to study the forced response of the flame in the channel while disconnecting the coupling with the acoustics of the channel. This can be done experimentally by changing the channel geometry upstream or downstream of the burner. Numerically, the same result can be achieved by diminishing the acoustic feedback of the channel to the burner, i.e., by using nonreflecting boundary conditions on inlets and outlets (Fig. 1b). This allows outgoing waves to leave the domain, but cancels the amplitude of waves entering the domain, thereby diminishing the possible effects of coupling mechanisms. In certain cases, making only the outlet nonreflecting (Fig. 1c) may be sufficient to stabilize the flow, as tested in Sec. V. There is no general rule indicating whether making boundaries nonreflecting in a given configuration will indeed be sufficient to damp the instability.

The decomposition of the Euler equations into characteristic waves is widely used to derive nonreflecting boundary conditions. A specific point that is common to all characteristic techniques is to prescribe the amplitude of the incoming waves.[3,5,13,14] The natural choice for nonreflecting boundaries is to set this amplitude to zero. This method is well suited to controlling the acoustic field (when acoustic waves reach the boundary at normal incidence) but not the mean flow: various authors[2,25] indicate that this choice may lead to ill-posed problems. Indeed, setting, for example, a zero amplitude for the incoming wave ($\mathcal{L}_1$) at a subsonic outlet (Fig. 2) may not allow the flow to retain a constant mean pressure. In the "real" world the mean pressure is imposed by the state at infinity downstream of the burner, where the pressure is P_∞, and this information is fed back into the domain through $\mathcal{L}_1$. Setting this value to zero is usually not a good choice because the information on P_∞ is simply ignored by the code, leading to possible drifts on the mean pressure. This problem is well known and various solutions have been proposed. One of them is to provide a value for $\mathcal{L}_1$, either using an analytical solution in region 2 or solving a linear problem between the outlet section S and infinity (see recent review edited by Tourrette and Halpern[26]). Such solutions can only be used in certain academic cases for which an analytical solution may be derived between the outlet of the computational domain and the "infinity" condition.[16] More practical (but less accurate) solutions have been proposed.

Received 16 April 2003; revision received 17 November 2003; accepted for publication 10 December 2003.

*Ph.D. Student, 42 avenue G. Coriolis; selle@cerfacs.fr.
†Professor, Math Department, ACSIOM Laboratory, CC51.
‡Research Director, UMR 5502, Allee du Professeur Camille Soula. Member AIAA.

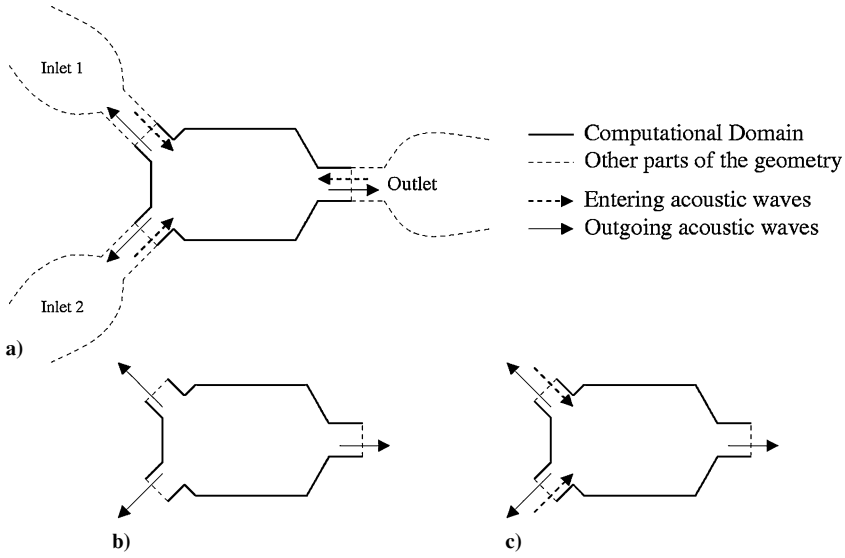

Fig. 1 Waves entering and leaving the computational domain.

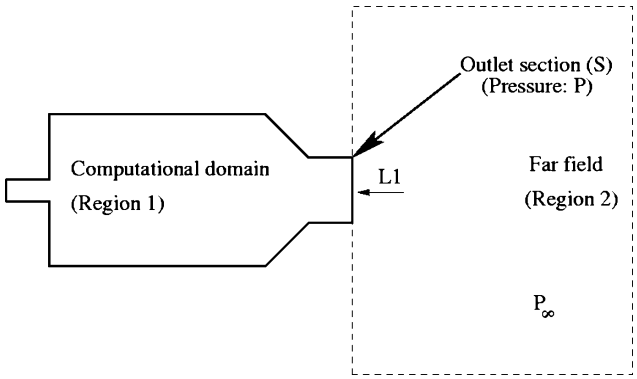

Fig. 2 Influence of far-field conditions on the amplitude of the waves entering the computational domain.

The simplest one (linear relaxation method; LRM) is to set the amplitude of $\mathcal{L}_1$ as proportional to the static pressure difference,[2,25] $\mathcal{L}_1 = K(P - P_\infty)$, where P is the predicted pressure at the outlet section S, P_∞ is the far field pressure, and K has the dimension of a frequency. "Appropriate" values of K are expected to provide a quasi-nonreflecting boundary condition while avoiding pressure drifts; if P drifts away from P_∞, $\mathcal{L}_1$ acts as a spring force to relax P toward P_∞.[27]

Even though this relaxation approach is used today in numerous studies,[28] two questions arise:

1) Are there optimal choices for K?

2) What is the effect of this relaxation on the global acoustic behavior of the boundary?

Obviously, low levels of K may be inefficient in terms of controlling the mean pressure. Conversely, high levels of K ensure that P remains very close to P_∞ and then make the boundary partially or fully reflecting. Therefore a direct link exists between the magnitude of K and the reflection coefficient R of the boundary. Actually K controls not only the magnitude of R but also its phase. Choosing K without care may lead to numerical results in which the outlet boundary condition introduces important biases in terms of acoustic behavior.

The objectives of this paper are 1) to derive a simple analytical solution relating the magnitude of the relaxation coefficient K and the complex reflection coefficient R of a boundary condition modeled with LRM (Sec. III); 2) to verify this relation using corresponding numerical simulations in which the outlet of a simple tube is submitted to a harmonic propagating wave (Sec. IV); 3) to demonstrate the effect of nonreflecting boundary conditions on the global resonance of a given duct using LRM, a simple case with fixed inlet velocity and nonreflecting LRM outlet is studied both analytically and numerically (Sec. V); and 4) finally, to propose a method to scale the K coefficient in practical computations (Sec. VI).

It will be shown that the values of K control the damping rate of the modes but may also change the eigenvalues significantly. In other words, a nonoptimal choice of K may lead to erroneous resonant frequencies.

II. Wave Amplitudes

The developments in this section are based on the method derived by Poinsot and Lele,[2] called Navier–Stokes characteristic boundary conditions (NSCBC). In all characteristic approaches the main issue is the determination of the amplitudes of waves entering the computational domain. In the NSCBC method the determination is based on the assumption that the amplitudes can be obtained as if the flow were laminar, one-dimensional, and inviscid (LODI). Note that for one-dimensional nonviscous flows, the NSCBC method is equivalent[26,29] to many other boundary treatments,[3,13,14,30] so that the results presented in Sec. III apply to all characteristic techniques using LRM.

LODI equations link the wave amplitudes ($\mathcal{L}_i$) and the temporal evolution of primitive Navier–Stokes variables (ρ, u, v, w, P). The wave amplitudes $\mathcal{L}_1, \mathcal{L}_2, \mathcal{L}_3, \mathcal{L}_4, \mathcal{L}_5$ correspond, respectively, to the left traveling acoustic wave (speed $u - c$), the entropy wave (speed u), the first vorticity wave (speed u), the second vorticity wave (speed u), and the right-traveling acoustic wave (speed $u + c$). Their expression is obtained through characteristic analysis[2,27]:

$$\frac{\partial \rho}{\partial t} + \frac{1}{c^2}\left[\mathcal{L}_2 + \frac{1}{2}(\mathcal{L}_5 + \mathcal{L}_1)\right] = 0 \tag{1}$$

$$\frac{\partial u}{\partial t} + \frac{1}{2\rho c}(\mathcal{L}_5 - \mathcal{L}_1) = 0 \tag{2}$$

$$\frac{\partial v}{\partial t} + \mathcal{L}_3 = 0 \tag{3}$$

$$\frac{\partial w}{\partial t} + \mathcal{L}_4 = 0 \tag{4}$$

$$\frac{\partial P}{\partial t} + \frac{1}{2}(\mathcal{L}_5 + \mathcal{L}_1) = 0 \tag{5}$$

where the wave amplitudes $\mathcal{L}_1, \ldots, \mathcal{L}_5$ are defined by

$$\mathcal{L}_1 = (u_1 - c)\left(\frac{\partial P}{\partial x_1} - \rho c \frac{\partial u_1}{\partial x_1}\right) \tag{6}$$

$$\mathcal{L}_2 = u_1\left(c^2 \frac{\partial \rho}{\partial x_1} - \frac{\partial P}{\partial x_1}\right) \tag{7}$$

$$\mathcal{L}_3 = u_1 \frac{\partial u_2}{\partial x_1} \tag{8}$$

$$\mathcal{L}_4 = u_1 \frac{\partial u_3}{\partial x_1} \tag{9}$$

$$\mathcal{L}_5 = (u_1 + c)\left(\frac{\partial P}{\partial x_1} + \rho c \frac{\partial u_1}{\partial x_1}\right) \tag{10}$$

Equations (1–5) provide a simple method to choose the incoming wave amplitudes to be imposed at a boundary. For example, from Eq. (2), a fixed velocity inlet condition will require the incoming wave amplitude $\mathcal{L}_5$ to be equal to the outgoing wave $\mathcal{L}_1$. Fixing a constant pressure at an outlet will be achieved [from Eq. (5)] by setting $\mathcal{L}_1 = -\mathcal{L}_5$. A more critical situation arises in mimicking nonreflecting conditions; this would require setting the incoming waves to zero. As indicated earlier, such a perfectly nonreflecting condition is not adequate because it may lead to a drift of the mean flow quantities. The next section illustrates the behavior of a duct outlet for which a nonreflecting condition is sought.

III. Reflection Coefficient of a Linear Relaxation Method Boundary Condition

Let us consider the propagation of one-dimensional acoustic waves in a semi-infinite tube of constant cross section (Fig. 3). The tube is infinite in the $x < 0$ direction and ends at $x = x_B$ in the other direction, where a nonreflecting boundary condition must be implemented. An harmonic wave propagating in increasing x direction is imposed. This wave amplitude is chosen so that in the absence of reflected wave, the inlet velocity signal would be $u(t) = U_0 e^{-i\omega t}$. Note that the phase is set to zero at $x = x_B$ to simplify the algebra. This has no influence on the result. The expression of this complex wave at $x = x_B$ is taken as

$$\mathcal{L}_5 = 2\rho c U_0 i\omega e^{-i\omega t} \tag{11}$$

The objective of the condition at $x = x_B$ is to be nonreflecting. In practice, to avoid a drift of the mean pressure, the incoming wave amplitude $\mathcal{L}_1$ is not set to zero but to

$$\mathcal{L}_1 = K(P - P_\infty) \tag{12}$$

Equations (11) and (12), together with LODI relations (2) and (5), lead to the system of equations

$$\frac{\partial u}{\partial t} + \frac{1}{2\rho c}(2\rho c U_0 i\omega e^{-i\omega t} - K(P - P_\infty)) = 0$$

$$\frac{\partial P}{\partial t} + \frac{1}{2}(2\rho c U_0 i\omega e^{-i\omega t} + K(P - P_\infty)) = 0 \tag{13}$$

The second equation of system (13) involves only P and can easily be solved. (This system was derived at the outlet boundary; consequently, coordinates are fixed and both u and P are functions of time only.) The solution for P is

$$P(t) = P_\infty + A_0 e^{-Kt/2} - \frac{\rho c U_0 i\omega}{K/2 - i\omega} e^{-i\omega t} \tag{14}$$

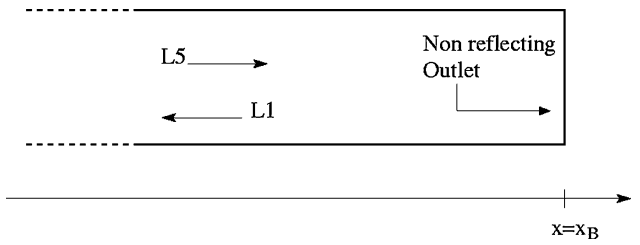

Fig. 3 One-dimensional harmonic wave impacting on the outlet boundary of a tube.

The transient term $A_0 e^{-Kt/2}$ of Eq. (14) (A_0 being a constant fixed by initial conditions) always vanishes with time since $K > 0$. In further developments it will be assumed that a steady state has been reached and this term will be omitted.

Equations (14) (without transient part) and (12) make it possible to reconstruct the incoming wave $\mathcal{L}_1$ and the complex reflection coefficient of the boundary. The analytical value of the reflection coefficient R is

$$R_{\text{out}} = \mathcal{L}_1/\mathcal{L}_5 = -1/[1 - i(2\omega/K)] \tag{15}$$

The magnitude $\|R\|$ and phase ϕ of a nonreflecting outlet modeled with LRM are derived from Eq. (15):

$$\|R\| = 1\Big/\sqrt{1 + (2\omega/K)^2} \tag{16}$$

$$\phi = -\pi - \arctan(2\omega/K) \tag{17}$$

The asymptotic behavior of $\|R\|$ and ϕ is summarized in Table 1.

As expected, for a given pulsation ω, $\|R\|$ goes to 0 when K is small, showing that the boundary condition is indeed nonreflecting ($\|R\| \simeq 0$) when K is limited to small values. However, large values of K destroy the nonreflecting character of the boundary condition: when K goes to infinity $\|R\|$ goes to 1, making the boundary fully reflecting. Actually, as shown by Eq. (16), the control parameter for $\|R\|$ is $2\omega/K$, so that one can define a cutoff pulsation $\omega_c = K/2$. For a fixed value of K (which is the case in any computation), all frequencies will not be reflected with the same strength. High frequencies will easily leave the computational domain ($R \to 0$), whereas very low frequencies will be strongly reflected ($R \to 1$). In practice a cutoff frequency f_c separates waves that will be reflected ($f < f_c$) from the ones that will leave the domain ($f > f_c$). f_c is defined from Eq. (15) by

$$f_c = \omega_c/2\pi = K/4\pi \tag{18}$$

This definition implies that $R(f_c) = 1/\sqrt{2}$. In terms of energy this means that at the frequency f_c half of the acoustic energy is fed back into the computational domain.

Figure 4 is a plot of Eqs. (6) and (17). The cutoff frequency f_c is represented by the vertical line. Equation (18) suggests that a proper interpretation of K is to view $f_c = K/(4\pi)$ as a frequency below which the boundary condition will not let the waves leave the domain.

Table 1 Asymptotic behavior of a nonreflecting outlet with LRM

Pulsation	$\|R\|$	ϕ
$\omega = 0$	1	$-\pi$
$\omega = K/2$	$1/\sqrt{2}$	$-\pi - \pi/4$
$\omega = \infty$	0	$-3\pi/2$

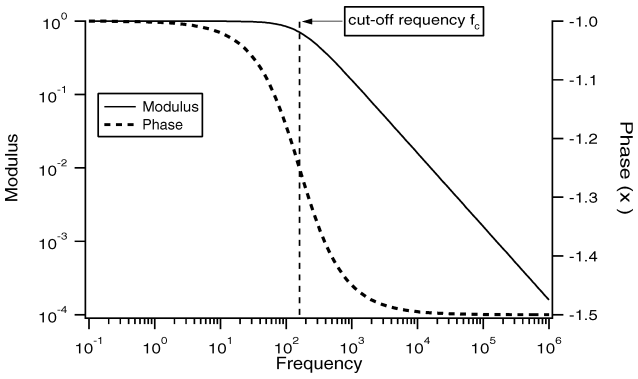

Fig. 4 Modulus and phase of reflection coefficient vs frequency at $K = 2000\ \text{s}^{-1}$.

Table 2 Summary of numerical simulation parameters

Parameter	Value
Size of the domain L, m	0.5
Number of cells	400
Mean inlet velocity, $m \cdot s^{-1}$	10
Sound speed c, $m \cdot s^{-1}$	348
Forcing frequency f, Hz	500
Forcing amplitude, $m \cdot s^{-1}$	0.1

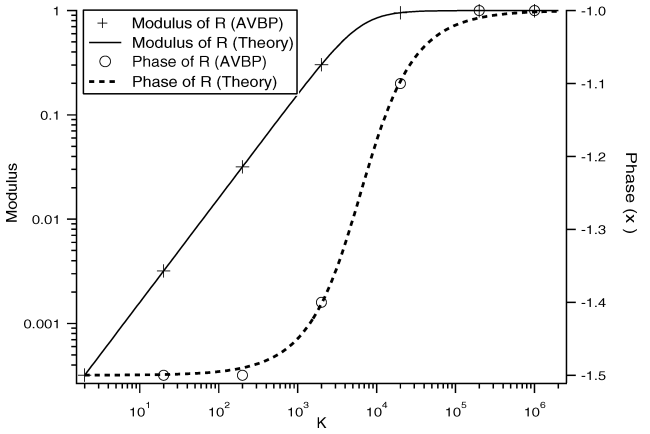

Fig. 5 Comparison of numerical and theoretical reflection coefficients at a "partially reflecting" outlet.

At constant K, the phase ϕ of the reflected signal is that of a fixed-pressure outlet for low values of ω. But as shown in Fig. 4, when the frequency increases, the boundary treatment induces a delay that moves the phase from $-\pi$ to $-3\pi/2$. This phase shift can induce dramatic changes in the acoustic properties of the domain, as shown in Sec. V.

IV. Numerical Evaluation of the Reflection Coefficient

In this section Eq. (15) is compared to numerical simulations. This is done by simply running a full Euler code on the configuration of Fig. 3 and using Eq. (12) at the outlet. The code AVBP was used for this validation. (The AVBP home page for detailed information is http://www.cerfacs.fr/cfd/CFDWeb.html.) AVBP is a three-dimensional fully compressible Navier–Stokes equation solver using characteristic boundary conditions.[2]

The outlet condition is nonreflecting (with LRM) as described in Sec. III and the inlet is a nonreflecting pulsed inlet.[31] The numerical scheme is second order in space and uses a three-step Runge–Kutta method (third order) for time integration. Calculation parameters are summarized in Table 2.

For technical reasons, it is more convenient to vary K at the outlet than to change the forcing frequency f at the inlet. Therefore the following results present $R(K)$ at fixed f instead of $R(f)$ at fixed K. The reflection coefficient R is obtained in AVBP by $R = \mathcal{L}_1/\mathcal{L}_5$. The amplitudes $\mathcal{L}_1$ and $\mathcal{L}_5$ are measured at the outlet using Eqs. (6) and (10) and one-sided spatial derivatives.

The agreement between numerical simulations and the theory [Eq. (15)] is extremely good (Fig. 5). Both modulus and phase of the reflection coefficient at the outlet are superimposed on the theoretical curves.

V. Computing a Closed Domain with Nonreflecting Boundary Condition

A. Description of the Configuration

The preceding sections have shown that nonreflecting boundary conditions using LRM can have impedances that make them partially reflecting. This section shows the implications of these results for the computation of flows where one or more sections are modeled using such nonreflecting conditions.

Consider a simple duct filled with a homogeneous gas (in which the speed of sound c is constant), as represented in Fig. 6. The inlet speed is imposed: $u(x=0,t)=U_0$. The steady flow solution is of course $u(x,t)=U_0$. This system is acoustically defined by its reflection coefficients at the inlet and the outlet. Assuming that the duct inlet is the phase reference, one can write the relations between the amplitude of the acoustic waves in the duct and the reflection coefficients:

$$R_{\text{in}} = \frac{\mathcal{L}_5}{\mathcal{L}_1}, \qquad R_{\text{out}} = \frac{\mathcal{L}_1 e^{-i\omega(L/c)}}{\mathcal{L}_5 e^{i\omega(L/c)}} \tag{19}$$

which can be written as

$$R_{\text{in}} R_{\text{out}} e^{i\omega(2L/c)} - 1 = 0 \tag{20}$$

Calculating the eigenfrequencies of this duct consists in giving the values of ω that are solutions of Eq. (20).

B. Analytical Solutions

For this test, the inlet corresponds to fixed velocity conditions, which implies that $R_{\text{in}} = 1$. The outlet is modeled using a nonreflecting condition with LRM. Therefore Eq. (15) shows that the effective impedance of this outlet is $R_{\text{out}} = -1/[1 - i(2\omega/K)]$. In this case Eq. (20) degenerates to

$$e^{i\omega(2L/c)} + [1 - i(2\omega/K)] = 0 \tag{21}$$

The values of ω that satisfy Eq. (21) are complex. The real part of ω ($\omega_r = \Re(\omega) = 2\pi f_r$) is the eigenpulsation and the imaginary part ($\omega_i = \Im(\omega) = 2\pi f_i$) is the damping (or amplification) rate. The temporal evolution of pressure and velocity at an eigenfrequency is proportional to $e^{-i\omega t} = e^{-i\omega_r t} e^{\omega_i t}$ (in the linear regime):

1) If $\omega_i > 0$, the mode is amplified: ω_r is an unstable pulsation.

2) If $\omega_i < 0$, the mode is damped: ω_r is a stable pulsation.

Figure 7 is a plot of the eigenfrequencies of Eq. (21) vs K. At very high values of K the system responds as if the pressure were fixed at the outlet. Combining Eqs. (11), (12), and (14) one can

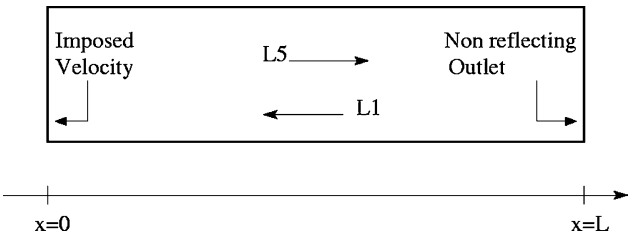

Fig. 6 Configuration.

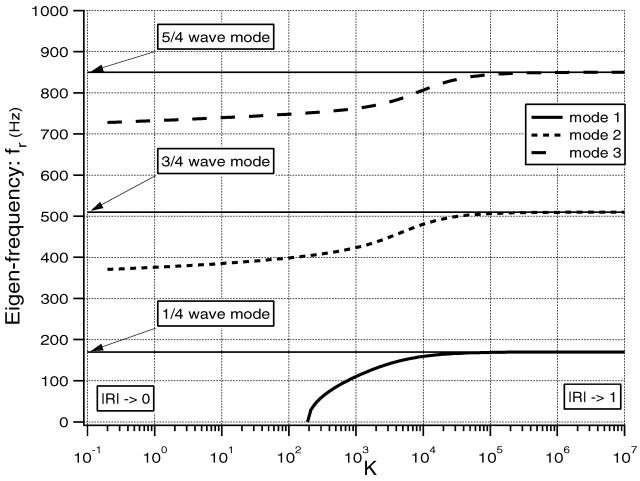

Fig. 7 Eigenfrequencies of the first three modes vs K for the duct of Fig. 6.

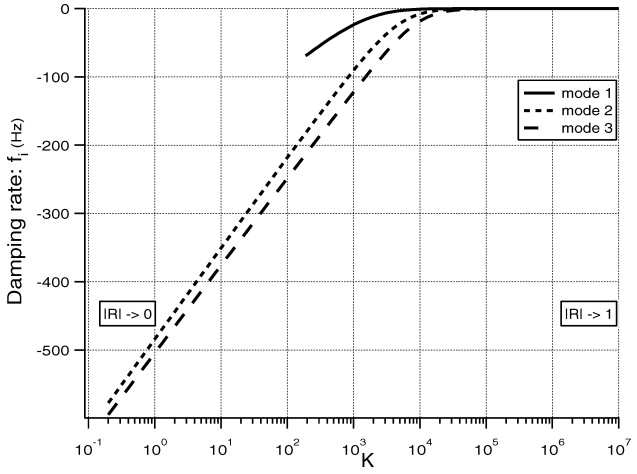

Fig. 8 Imaginary part of the first three modes vs K for the duct of Fig. 6.

show that $\mathcal{L}_5 + \mathcal{L}_1$ goes to zero when K goes to infinity, and the eigenfrequencies

$$f_n = (2n+1)(c/4L) \tag{22}$$

correspond directly to the $\frac{1}{4}$ wave ($n=0$), $\frac{3}{4}$ wave ($n=1$), ... modes of a duct with fixed inlet velocity and outlet pressure (represented by horizontal lines in Fig. 7): the boundary is fully reflecting.

When K decreases the eigenfrequencies of the duct also decrease due to the phase shift induced by the boundary treatment shown by Eq. (17). At very low K values the 1/4 wave mode even disappears.

At very high values of K the imaginary part f_i of all eigenfrequencies is zero (Fig. 8), indicating that they are not damped. This is consistent with the fact that there is no source term in the duct and boundary conditions are acoustically closed (no fluctuation of P or u allowed). Obviously at such large K values the outlet boundary condition fails to evacuate acoustic waves. For lower values of K the modulus of R_{out} is lower than 1 and thus all modes are damped ($\Im(\omega) < 0$).

Figures 7 and 8 show that the value of K must remain small to provide damped modes but also that the modes that appear are not physical: their frequencies are not the eigenfrequencies of the duct.

VI. Scaling Strategy for the Relaxation Coefficient K

As shown in the preceding sections, the value of K has a drastic influence on the results of a numerical simulation. This has already been pointed out by different authors for either steady[25] or unsteady[2] calculations. The main problem for several authors is to know how to choose K in practical cases. Rudy and Strikwerda[25] suggested the following scaling of K for optimal convergence of steady calculations:

$$K = \sigma(1-\mathcal{M}^2)(c/L) \tag{23}$$

where $\mathcal{M}$ is the Mach number of the mean flow, c the sound speed, and L the domain size.

Numerical simulations[2,25,27] showed that an optimum is reached for $\sigma_{\text{Num}}^{\text{optim}} = 0.58$, whereas the theory of Rudy and Strikwerda[25] suggested an optimum value of $\sigma_{\text{RS}}^{\text{optim}} = 0.27$. Rudy and Strikwenda's definition of the optimum value for σ is based on the convergence of steady-state calculations, whereas in Refs. 2 and 27 the definition is based on both the convergence of mean values and the evacuation of acoustic waves in unsteady calculations.

The present work gives a new interpretation of K, which is now linked to the cutoff frequency of the boundary by Eq. (18). Thus "good" values of K are those that allow all duct acoustic modes to leave the domain. It was shown in Sec. III that frequencies lower than $f_c = K/(4\pi)$ are reflected, and frequencies higher than f_c leave the computational domain. It is then relevant to choose K so that f_c is lower than all acoustic frequencies expected in the computational domain.

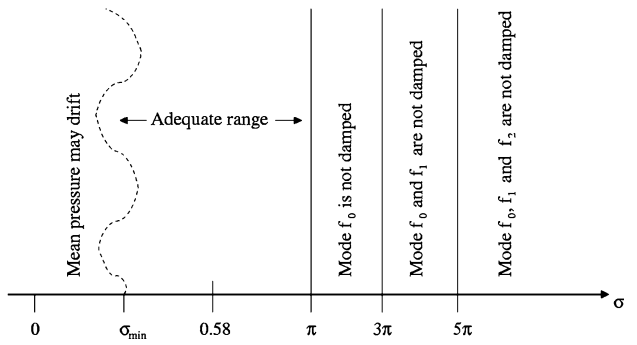

Fig. 9 Summary of the influence of σ on the acoustics and mean flow quantities.

As an example, this strategy is now applied to the duct of Sec. V. Since velocity is imposed at the inlet and pressure at the outlet, the lowest acoustic frequency is that of a quarterwave mode. At a given Mach number $\mathcal{M}$ the quarter wave mode frequency is

$$f_0 = (1-\mathcal{M}^2)(c/4L) \tag{24}$$

From Eqs. (18) and (24) the highest value of K for this calculation that will significantly damp the 1/4 wave mode (as well as other higher order modes) is

$$K^{\max} = \pi(1-\mathcal{M}^2)(c/L) \tag{25}$$

This scaling of K is very similar to the theory of Rudy and Strikwerda[25] given in Eq. (23) but with a σ coefficient of π instead of 0.58. This approach suggests that the highest admissible value of σ to prevent acoustic feedback is

$$\sigma^{\max} = \pi \tag{26}$$

On the other hand, K (or σ) has to be chosen large enough to prevent a drift in the mean values (pressure, mass flow, etc.). Figure 9 offers a simple summary of these findings. (Note that Fig. 9 is actually a one-dimensional plot.) The minimum admissible value $\sigma_{\min}$ is not fixed by acoustics. It strongly depends on the computational parameters (Reynolds number, three-dimensional effects such as swirl and geometry, etc.). Consequently, the boundary $\sigma_{\min}$ is not clearly defined in Fig. 9. Other tests (not reported here) suggest that choosing σ lower than 0.1 often increases convergence times and sometimes does not allow mass fluxes and pressure to reach a steady state.

VII. Numerical Computations

Section V.B has provided a theoretical stability analysis of the duct of Fig. 6. In the present section, these results are tested numerically. The duct inlet is a fully reflecting characteristic inlet with imposed velocity, achieved through LODI relation 2 by imposing $\mathcal{L}_5 = \mathcal{L}_1$. A nonreflecting outlet with LRM is applied at the outlet; the value of σ is varied to illustrate the results of Secs. V and VI. A Gaussian perturbation is superimposed on the initial pressure field to excite all acoustic modes.

Two values for σ are investigated to illustrate the influence on both the damping of acoustics and the shift of the eigenfrequencies of the duct.

A. Case 1: $\sigma = 10\pi$

In this section, the relaxation factor at the outlet σ is fixed to $\sigma = 10\pi$, which is too high to evacuate the first eigenmodes of the duct. The pressure perturbations recorded at the inlet show exponential decay (Fig. 10) before $t = 0.1s$, corresponding to the evacuation of high-frequency modes. The signal then remains almost constant, because low-frequency modes are reflected by the outlet condition.

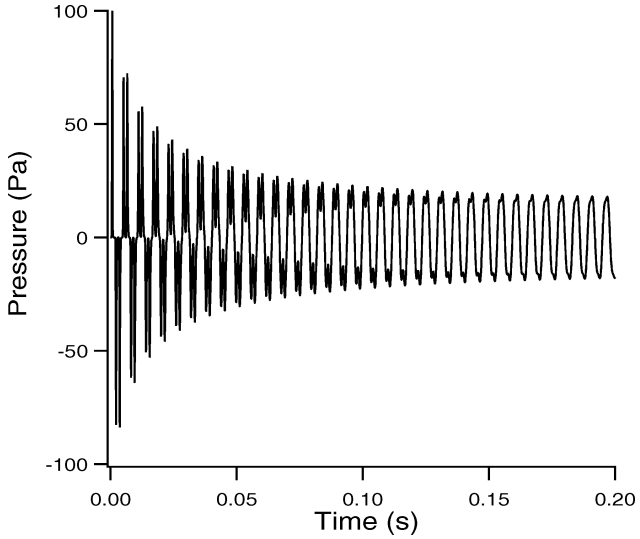

Fig. 10 Time evolution of pressure perturbation at the inlet ($\sigma = 10\pi$).

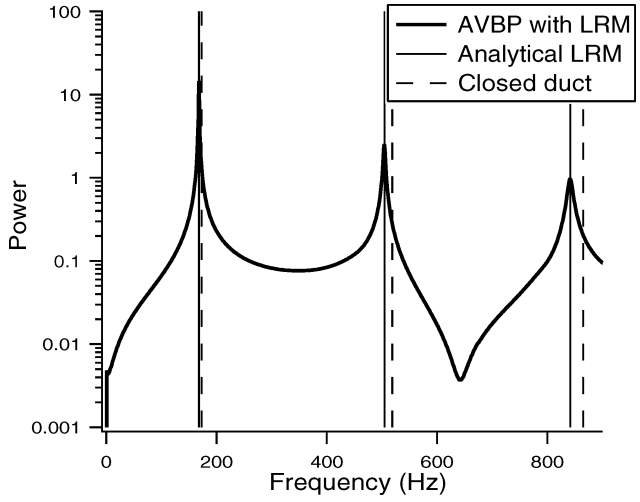

Fig. 11 Spectrum of pressure signal ($\sigma = 10\pi$) compared to analytical values of Sec. V and Eq. (22).

Figure 11 is the Fourier transform of the inlet pressure signal. The spectrum is compared to the expected eigenfrequencies analytically derived in Sec. V. The first three modes predicted by Eq. (21) and displayed in Fig. 11 remain in the computational domain, as suggested from Fig. 9 for $\sigma = 10\pi$. Moreover, the frequencies of these modes are not the true eigenfrequencies as predicted by Eq. (22), which gives the eigenfrequencies of an acoustically closed duct (imposed velocity at the inlet and imposed pressure at the outlet). This confirms the biasing effects induced by the outlet condition when large values of σ are used:

1) The outlet is strongly reflecting, so that certain modes are not damped.

2) The frequencies of the modes differ from the true eigenfrequencies of the duct.

Obviously, this would not be a good choice for σ for practical computations.

The agreement between numerical and analytical results is good; the shift between the eigenfrequencies of the closed duct and the duct with LRM is correctly predicted.

B. Case 2: $\sigma = \pi$

In this section the relaxation factor σ is set to π, which is the highest value that enables the evacuation of all acoustic modes of the duct.

Figure 12 shows the exponential decay of the pressure perturbations. At $t = 0.1$s all acoustic modes have vanished. Note that there

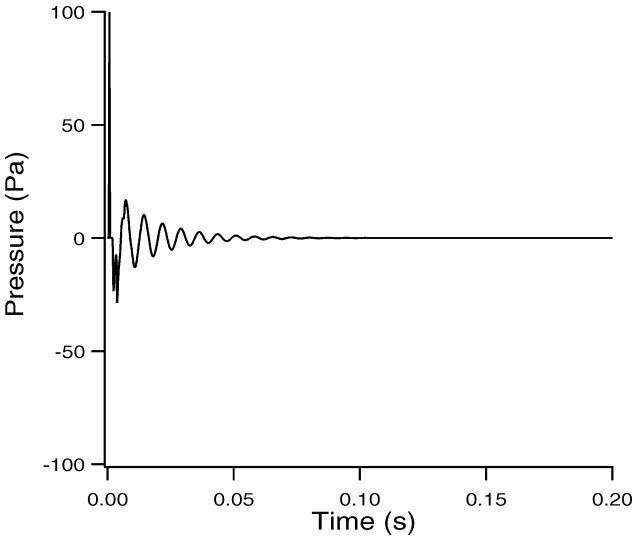

Fig. 12 Time evolution of pressure perturbation at the inlet ($\sigma = \pi$).

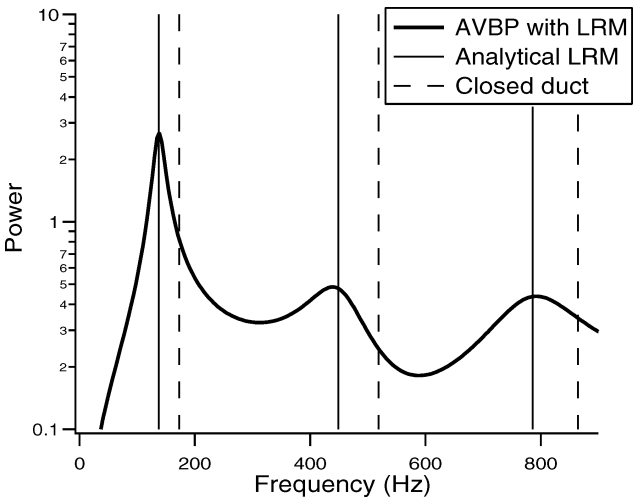

Fig. 13 Spectrum of pressure signal ($\sigma = \pi$) compared to analytical values of Sec. V and Eq. (22).

is no source term in the domain and that the simulation is quite long compared to f_c (35 cycles), so that even a reflection coefficient slightly lower than 1 (the definition of the cutoff frequency f_c is that $R = 1/\sqrt{2}$) attenuates the mode.

Figure 13 is the Fourier transform of the pressure signal of Fig. 12 between $t = 0$ and 0.05s. The spectrum is compared to the expected eigenfrequencies analytically derived in Sec. V and to the true eigenfrequencies of the duct given by Eq. (22). The spectrum is not very sharp, due to the exponential decay of the signal, and yet the agreement is fairly good. Again the eigenfrequencies of the duct are significantly shifted compared to those of an acoustically closed duct.

VIII. Conclusions

A simple acoustic theory was proposed to characterize the actual reflection coefficient of numerical "nonreflecting" boundary conditions using LRM (linear relaxation method) as proposed by Rudy and Strikwerda[25] or Poinsot and Lele.[2] It has been shown that large values of the relaxation coefficient K used in these methods to link the ingoing wave amplitude $\mathcal{L}_1$ to the pressure difference $(P - P_\infty)$ make the boundary condition fully reflecting and that K can be linked to a cutoff frequency f_c by $K = 4\pi f_c$. At a given value of K, all modes such that $f < f_c$ are not damped. A proper strategy to minimize acoustic coupling is to choose K such that f_c is lower than the first duct acoustic mode. In the case of a

one-dimensional duct with imposed velocity inlet, this is obtained by writing $K = \sigma(1 - \mathcal{M}^2)(c/L)$ and choosing $0.2 < \sigma < \pi$. For more complex cases (three dimensions, complex geometries, combustions, etc.), an extension of this strategy is to solve the general acoustic equation in the domain to find its eigenfrequencies f_i. The maximum value of σ is then given by choosing $f_c = \min(f_i)$.

References

[1]Engquist, B., and Majda, A., "Absorbing Boundary Conditions for the Numerical Simulation of Waves," *Mathematics of Computations*, Vol. 31, 1977, pp. 629–651.

[2]Poinsot, T., and Lele, S., "Boundary Conditions for Direct Simulations of Compressible Viscous Flows," *Journal of Computational Physics*, Vol. 101, No. 1, 1992, pp. 104–129.

[3]Hirsch, C., *Numerical Computation of Internal and External Flows*, Vol. 2, Wiley, New York, 1988, Chap. 19.

[4]Hagstrom, T., and Hariharan, S. I., "Accurate Boundary Conditions for Exterior Problems in Gas Dynamic," *Mathematics of Computation*, Vol. 51, 1988, pp. 581–597.

[5]Tourrette, L., "Artificial Boundary Conditions for the Linearized Compressible Navier–Stokes Equations," *Journal of Computational Physics*, Vol. 137, 1997, pp. 1–37.

[6]Hayder, M. E., and Turkel, E., "Nonreflecting Boundary Conditions for Jet Flow Computations," *AIAA Journal*, Vol. 33, 1995, pp. 2264–2270.

[7]Tsynkov, S. V., "Numerical Solution of Problems on Unbounded Domains: A Review," *Applied Numerical Mathematics*, Vol. 27, 1998, pp. 465–532.

[8]Vasilyev, O. V., and Bowman, C., "Second-Generation Wavelet Collocation Method for the Solution of Partial Differential Equations," *Journal of Computational Physics*, Vol. 165, No. 2, 2000, pp. 660–693.

[9]Kim, J. W., and Lee, D. J., "Generalized Characteristic Boundary Conditions for Computational Aeroacoustics," *AIAA Journal*, Vol. 38, 2000, pp. 2040–2049.

[10]Colonius, T., Lele, S., and Moin, P., "Boundary Conditions for Direct Computation of Aerodynamic Sound Generation," *AIAA Journal*, Vol. 31, No. 9, 1993, pp. 1574–1582.

[11]Rowley, C. W., and Colonius, T., "Discretely Nonreflecting Boundary Conditions for Linear Hyperbolic Systems," *Journal of Computational Physics*, Vol. 157, 2000, pp. 500–538.

[12]Freund, J. B., "Proposed Inflow/Outlow Boundary Condition for Direct Computation of Aerodynamic Sound," *AIAA Journal*, Vol. 35, 1997, pp. 740–742.

[13]Thompson, K. W., "Time Dependent Boundary Conditions for Hyperbolic Systems," *Journal of Computational Physics*, Vol. 68, 1987, pp. 1–24.

[14]Thompson, K. W., "Time Dependent Boundary Conditions for Hyperbolic Systems," *Journal of Computational Physics*, Vol. 89, 1990, pp. 439–461.

[15]Grappin, R., Lorat, J., and Buttighoffer, A., "Alfvén Wave Propagation in the High Sonar Corona," *Astronomy and Astrophysics*, Vol. 362, 2000, pp. 342–358.

[16]Barry, A., Bielak, J., and MacCamy, R. C., "On Absorbing Boundary Conditions for Wave Propagation," *Journal of Computational Physics*, Vol. 79, 1988, pp. 449–468.

[17]Mur, G., "Absorbing Boundary Conditions for the Finite-Difference of the Time-Domain Electromagnetic-Field Equations," *IEEE Transactions on Electromagnetic Compatibility*, Vol. 23, 1981, pp. 377–382.

[18]Ho, C. M., and Huerre, P., "Perturbed Free Shear Layers," *Journal of Fluid Mechanics*, Vol. 16, 1984, pp. 365–424.

[19]Lucas, L., and Rockwell, D., "Self-Excited Jet: Upstream Modulation and Multiple Frequencies," *Journal of Fluid Mechanics*, Vol. 147, 1984, pp. 333–352.

[20]Crighton, D. G., Dowling, A., Heckl, M., Leppington, F., and Williams, J., *Modern Methods in Analytical Acoustics*, Springer-Verlag, Berlin, 1992, Chap. 13.

[21]Yang, V., and Culick, F. E. C., "Analysis of Low-Frequency Combustion Instabilities in a Laboratory Ramjet Combustor," *Combustion Science and Technology*, Vol. 45, 1986, pp. 1–25.

[22]Poinsot, T., Trouvé, A., Veynante, D., Candel, S., and Esposito, E., "Vortex Driven Acoustically Coupled Combustion Instabilities," *Journal of Fluid Mechanics*, Vol. 177, 1987, pp. 265–292.

[23]McManus, K., Poinsot, T., and Candel, S., "A Review of Active Control of Combustion Instabilities," *Progress in Energy and Combustion Science*, Vol. 19, 1993, pp. 1–29.

[24]Angelberger, C., Egolfopoulos, F., and Veynante, D., "Large Eddy Simulations of Chemical and Acoustic Effects on Combustion Instabilities," *Flow Turbulence and Combustion*, Vol. 65, No. 2, 2000, pp. 205–222.

[25]Rudy, D. H., and Strikwerda, J. C., "A Non-Reflecting Outflow Boundary Condition for Subsonic Navier–Stokes Calculations," *Journal of Computational Physics*, Vol. 36, 1980, pp. 55–70.

[26]Tourrette, L., and Halpern, L., *Absorbing Boundaries and Layers, Domain Decomposition Methods: Applications to Large Scale Computation*, Nova Science, Huntington, NY, 2001.

[27]Poinsot, T., and Veynante, D., *Theoretical and Numerical Combustion*, R. T. Edwards, Flourtown, PA, 2001.

[28]Wall, C., Pierce, C. D., and Moin, P., "A Semi-Implicit Method for Resolution of Acoustic Waves in Low Mach Number Flows," *Journal of Computational Physics*, Vol. 181, 2002, pp. 545–563.

[29]Nicoud, F., "Defining Wave Amplitude in Characteristic Boundary Conditions," *Journal of Computational Physics*, Vol. 149, No. 2, 1998, pp. 418–422.

[30]Giles, M., "Non-Reflecting Boundary Conditions for Euler Equation Calculations," *AIAA Journal*, Vol. 28, No. 12, 1990, pp. 2050–2058.

[31]Kaufmann, A., Nicoud, F., and Poinsot, T., "Flow Forcing Techniques for Numerical Simulation of Combustion Instabilities," *Combustion and Flame*, Vol. 131, 2002, pp. 371–385.

S. Mahalingam
Associate Editor